

# Diffusion-driven current transport to near-surface nanostructures

Pyry Kivisaari<sup>1</sup>, Lauri Riuttanen<sup>2</sup>, Sami Suihkonen<sup>2</sup>, and Jani Oksanen<sup>3</sup>

<sup>1</sup>Nanometer Structure Consortium, Lund University, P.O. Box 118, SE-22100 Lund, Sweden

<sup>2</sup>Department of Micro- and Nanosciences, Aalto University, P.O. Box 13000, FI-00076 Aalto, Finland

<sup>3</sup>Department of Biomedical Engineering and Computational Science, Aalto University, P.O. Box 12200, FI-00076 Aalto, Finland  
Email: pyry.kivisaari@ftf.lth.se

**Abstract**—Diffusion-driven current transport (DDCT) has recently been proposed as a new way to organize the current injection in nanoscale optoelectronic devices. The very recent first proof-of-principle experiments have also shown that DDCT works as predicted theoretically. In this work we perform simulations on DDCT-based III-Nitride devices and demonstrate how the optimization of DDCT differs significantly from the optimization of conventional double heterostructure based devices.

## I. INTRODUCTION

Nanostructures provide many potential advantages for next-generation photonic devices due to, e.g., the possibility to enhance light extraction/absorption [1] and the improved opportunity to integrate radiative III-V materials directly with electronics [2]. However, the conventional double heterostructure based current transport method presents large challenges for developing efficient and functional nanostructure devices. To remedy this problem and provide new nanodevice design opportunities, we recently proposed a diffusion-driven current transport (DDCT) concept to excite surface nanostructures [3]. The first experimental proof-of-principle structures showed that the concept works in buried and near-surface InGaN quantum wells (QWs) as predicted by theory. The first experiments also revealed some of the peculiar properties of DDCT, such as the positive correlation between efficiency and temperature [4]–[6].

However, the first theoretical and experimental works merely showed that the DDCT works as expected from current transport simulations. Substantial efforts in theoretical modeling and experimental work are still needed to disentangle the most interesting opportunities presented by DDCT and to produce efficient DDCT-based devices. In this work we model the operation of the prototype DDCT-based III-N structures illustrated in Fig. 1 to demonstrate how the injection efficiency depends on the design parameters of the structure. Our results show that the optimization of DDCT-based structures differs significantly from optimization of typical solid-state light emitting devices.

## II. THEORY

Diffusion-driven current transport is simulated in a 2D cross-section along the  $xy$  plane of the structures of Fig. 1. The simulations are carried out using the drift-diffusion (DD)

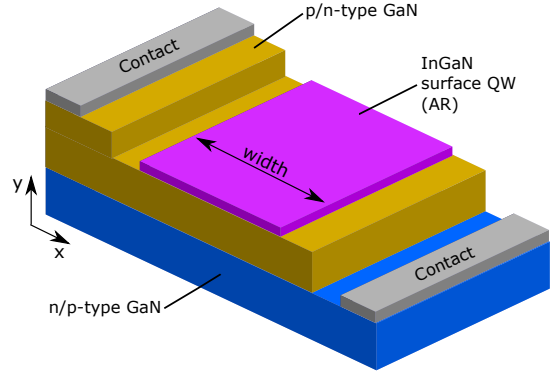


Fig. 1. Schematic figure of the structures simulated in this work. Note that the dimensions are not in scale. The structure with n-type GaN on the bottom is referred to as n-DDLED, and the structure with p-type GaN on the bottom is conversely p-DDLED.

model, given by [7]

$$\begin{aligned} \nabla \cdot (-\varepsilon \nabla \phi + \mathbf{P}_{tot}) &= e(p - n + N_d - N_a) \\ \nabla \cdot \mathbf{J}_n &= \nabla \cdot (\mu_n n \nabla E_{Fn}) = eR \\ \nabla \cdot \mathbf{J}_p &= \nabla \cdot (\mu_p p \nabla E_{Fp}) = -eR, \end{aligned} \quad (1)$$

where  $\varepsilon$  is the permittivity,  $\phi$  is the electrostatic potential,  $\mathbf{P}_{tot}$  includes spontaneous and piezoelectric polarizations,  $e$  is the elementary charge,  $n$  and  $p$  are electron and hole densities,  $N_{d,a}$  are the ionized donor and acceptor doping densities,  $\mathbf{J}_{n,p}$  are the electron and hole current densities,  $\mu_{n,p}$  are the electron and hole mobilities,  $E_{Fn,Fp}$  are the quasi-Fermi levels for the conduction and valence bands, and  $R$  is the net recombination rate density. Recombination is calculated by accounting for the Shockley-Read-Hall (SRH), radiative, and Auger recombinations using parametrized models based on the carrier densities. Further details of the simulation model as well as the material parameters can be found in Ref. [8].

As illustrated in Ref. [5], the injection efficiency of DDCT-based structures depends heavily on the doping densities, layer thicknesses and the areas of the InGaN active region (AR) and contacts. We simulate current transport in the n-DDLED structure with different areas of the AR by varying the width marked in Fig. 1. In the p-DDLED structure, we study by simulations how the injection efficiency and current-voltage characteristics depend on  $N_d$  in the n-type layer between the AR and the pn junction.

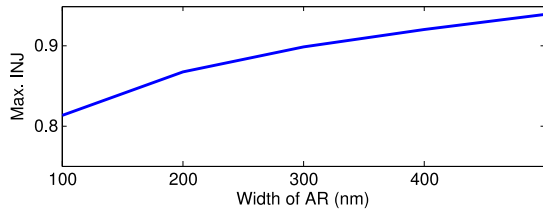


Fig. 2. Maximum injection efficiency of the n-DDLED structure as a function of the total width of the active region.

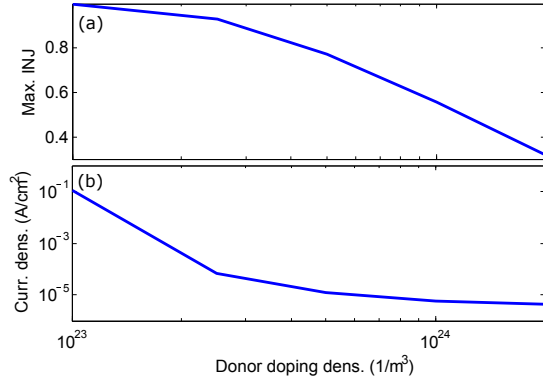


Fig. 3. (a) Maximum injection efficiency and (b) current density at a bias voltage of 2.7 V in the p-DDLED structure as a function of  $N_d$  in the GaN layer between the AR and the p-type GaN.

### III. RESULTS

Figure 2 shows the maximum injection efficiency of the n-DDLED structure as a function of the width of the AR. As expected from analytical models [5], the injection efficiency of the n-DDLED structure approaches unity as the width of the AR increases while the contact area remains unchanged. Another way to optimize the injection efficiency of n-DDLED would be by decreasing the thickness of the layer between the AR and the pn junction in the  $y$  direction.

Figure 3(a) shows the maximum injection efficiency of the p-DDLED structure as a function of  $N_d$  in the layer between the AR and the pn junction. As explained in Ref. [5], donor doping increases the potential barrier for holes between the p-type region and the AR. The injection efficiency reaches unity in the p-DDLED structure at an ionized donor density of  $10^{23}$   $1/m^3$ . Figure 3(b) shows the current density of the p-DDLED at a bias voltage of 2.7 V as a function of the ionized donor density. Somewhat counterintuitively, the current density decreases at 2.7 V by increasing the donor density, but this results from the fact that the potential barrier for holes increases with  $N_d$  and blocks hole current to the AR. Increasing  $N_d$  increases the electron leakage current which, however, is still small at 2.7 V and becomes significant only at bias voltages comparable to the built-in potential (3.28 V).

The effect of  $N_d$  in the p-DDLED structure can be further illustrated by looking at the band diagrams. Figure 4 shows the band diagrams of the p-DDCT structure with a donor doping of (a)  $10^{23}$   $1/m^3$  and (b)  $2.5 \times 10^{23}$   $1/m^3$  at a bias voltage of 2.7 V. The band diagrams are plotted in the middle of the structure in Fig. 1 in the  $y$  direction, starting from the bottom and ending at the top of the AR. The band diagram in (a) shows that the potential barrier for holes is small due to the relatively small

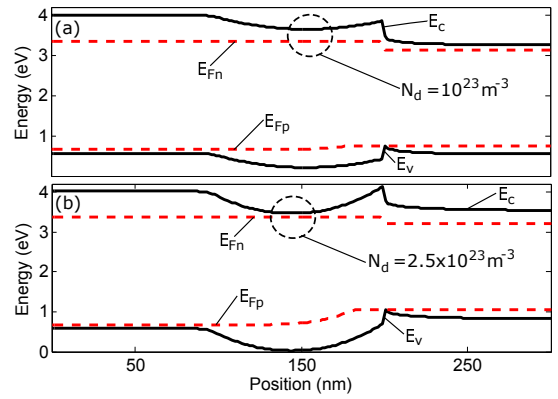


Fig. 4. Band diagrams of the p-DDLED structure with a donor doping of (1)  $10^{23}$   $1/m^3$  and (b)  $2.5 \times 10^{23}$   $1/m^3$  at a bias voltage of 2.7 V, plotted in the middle of the structure from bottom to top.

donor doping in the n-type GaN. Therefore the hole current flow through the n-GaN layer is not restricted as indicated by the very small change in the valence band quasi-Fermi level. However, even the quasi-Fermi level of electrons suffers only a small decrease at the interface of the AR, indicating also efficient electron transport to the AR. The band diagram in (b) shows that the increased donor doping creates a larger potential barrier for holes, resulting in the large change in the valence band quasi-Fermi level. The quasi-Fermi level for electrons decreases roughly by the same amount in (a) and (b) due to the negative polarization charge at the interface.

### IV. CONCLUSIONS

We performed current transport simulations in III-N structures to demonstrate how the optimization of DDCT-based optoelectronic devices differs from more conventional optoelectronic devices. Further understanding and developing the structures and materials of DDCT-based devices requires close collaboration between experiment and theory.

### ACKNOWLEDGMENTS

We acknowledge the Aalto Energy Efficiency Programme (AEF), the Academy of Finland, and the Nokia Foundation for support.

### REFERENCES

- [1] J. Wallentin, N. Anttu, D. Asoli, M. Huffman, I. Åberg, M. H. Magnusson, G. Siefert, P. Fuss-Kailuweit, F. Dimroth, B. Witzigmann, H. Q. Xu, L. Samuelson, K. Deppert, and M. Borgström, *Science* **339**, 1057–1060 (2013).
- [2] K. Tomioka, M. Yoshimura, and T. Fukui, *Nature* **588**, 189–192 (2012).
- [3] P. Kivisaari, J. Oksanen, and J. Tulkki, *Appl. Phys. Lett.* **103**, 031103 (2013).
- [4] L. Riuttanen, P. Kivisaari, H. Nykänen, O. Svensk, S. Suihkonen, J. Oksanen, J. Tulkki, and M. Sopanen, *Appl. Phys. Lett.* **104**, 081102 (2014).
- [5] L. Riuttanen, P. Kivisaari, O. Svensk, J. Oksanen, and S. Suihkonen, *IEEE T. Electron Dev.* **62**, 902–908 (2015).
- [6] L. Riuttanen, P. Kivisaari, O. Svensk, J. Oksanen, and S. Suihkonen, submitted for publication (2015).
- [7] J. Piprek, S. Li in *Optoelectronic Devices: Advanced Simulation and Analysis*, edited by J. Piprek (Springer, New York, 2005).
- [8] P. Kivisaari, J. Oksanen, and J. Tulkki, *J. Appl. Phys.* **111**, 103120 (2012).